**Revista Boliviana de Química, 2025, Vol. 42, N°2, 121-132**
Natalie N. Escobar-Flores et al.
https://doi.org/10.53287/xfdg4218co50i

*Original article* [1]

# Isolation of rutin and 2-nonanone from *Ruta graveolans; 2-Non*'s calculated and experimental $^{1}H$, $^{13}C$ NMR spectra compared

**Natalie N. Escobar-Flores, Santiago Tarqui, José A. Bravo, José L. Vila***

Instituto de Investigaciones Químicas IIQ-NatProd, Universidad Mayor de San Andrés UMSA, Av. Villazón N° 1995, La Paz, Bolivia

**Keys:** *NMR spectra, Spartan 18 Software, 2-Nonanone, rutin, Ruta graveolans;* **Claves:** *Espectros de RMN, Software Spartan 18, 2-Nonanona, rutina, Ruta graveolans.*

## ABSTRACT

The isolation of rutin (1) and 2-Nonanone (2) from the species *Ruta* graveolans is reported. Structural identification was performed by $^{1}H$ and $^{13}C$ NMR spectroscopy. The structural parameters of 2-nonanone were determined by B3LYP with the 6-31G* basis set. The results of the optimized molecular structure are presented by comparing the calculated values with experimental spectral data. Theoretical quantum calculations resulted in a good predictive structure determination approach for the 2-nonanone molecule.

.

## RESUMEN

*Aislamiento de rutina y 2-nonanona de Ruta graveolans; comparación de espectros de RMN de 1H, 13C calculados y experimentales de 2-Non*. Se reporta el aislamiento de rutina (**1**) y 2-Nonanona (**2**) de la especie *Ruta graveolans*. La identificación estructural fue realizada mediante espectroscoía de RMN de $^{1}H$ y $^{13}C$. Los parámetros estructurales de la 2-nonanona se determinaron mediante B3LYP con el conjunto base 6-31G*. Se presentan los resultados de la estructura molecular optimizada comparando los valores calculados con los datos espectrales experimentales. Los cálculos cuánticos teóricos dieron como resultado un buen enfoque de determinación estructural predictiva para la molécula 2-nonanona.

**Revista Boliviana de Química, 2025, 42, 121-132**
**ISSN 0250-5460, Rev. Bol. Quim.** ***Paper edition***
**ISSN 2078-3949, Rev. boliv. quim.** ***e-edition*****,** ***May-Nov***
**30 noviembre 2025,** https://doi.org/10.53287/xfdg4218co50i

https://bolivianchemistryjournaliiq.umsa.bo

[1]Received June 14, 2025, accepted October 27, 2025, published November 30, 2025. *Mail to: jvila@fcpn.edu.bo

## INTRODUCTION

*Ruta graveolans* (*Ruta*ceae) cultivated and wild species, is found in the high valleys of the La Paz region and is used in traditional Bolivian medicine, as reported in the book "Kallawaya" (Traveling Healers of the Andes). This plant species is known by different names, depending on the native language: Quirupichana (Quechua), Chchapi-chchapi (Aymara), *Ruta-Ruta* (Kallawaya), and is used as an antispasmodic, antirheumatic, vermifuge, and sudorific.[1]

The traditional medicinal uses of *Ruta* species are primarily as an abortifacient and emmenagogue, and in the treatment of lung diseases and microbial infections.[2] [3] To treat common illnesses, rural and urban communities in Bolivia currently use traditional medicine, which is a fundamental part of daily life. *Ruta* is used in the form of an infusion, poultice, or direct application. *Ruta* is used as the leaves, branches, or the whole plant.[4]

*Ruta* species present essential oils in the aerial part, essential oils have been reported in fresh and dried plants, the essential oils reported in *Ruta* species are; 2-undecanone, 2-nonanone, 2-dodecanone, 2-decanone as the main components of *Ruta* essential oils, these chemical compounds are the result of the study of 66 *Ruta* species. However, 2-undecanol acetate, 2-methylbutyl ester of 2-undecanol, menthol, linalool, 2-hexanal, limonene and β-caryophyllene have also been reported.[5] Other studies of oils have also been carried out, having reported geijerene, octyl acetate, methyl decanoate and phytyl acetate.[6] [7]

The common presence of the compound 2-undecanone in all *Ruta* species shows it to be the main compound in *Ruta* essential oils. This compound has been identified as a suitable chemotaxonomic marker for the *Ruta* genus. However, for the same reason, 2-nonanone could also be another marker compound for the chemotaxonomic study of the *Ruta* genus.[5] [8] The main bioactivities of *Ruta* essential oils are anti-inflammatory, antimicrobial, antioxidant, antiprotozoal, cytotoxic, herbicidal, insecticidal, insect repellent, larvicidal, nematocidal/anthelminthic, and phytotoxic properties. However, the main potential of essential oils of the *Ruta* genus lies in their pesticidal, larvicidal, insecticidal, and insect repellent properties, which can be applied to the development of commercial agrochemical products. [5]

Rutin (**1**) chemically, is a phenolic compound whose aglycone is a flavonol of 15 carbon atoms, which is the base structure of flavonoids consisting of three rings, two aromatic rings (ring A and B), which are linked to a three-carbon chain that forms the third ring (ring C), are arranged as C6-C3-C6 called quercetin and is linked to a glycoside which is the disaccharide rhamnosylglucose (3,3',4',5,7-pentahydroxyflavone-3-rhamnoglucoside), this molecule is also known as rutoside, quercetin-3-rutenoside and sophorine. rutin is a natural compound present in various plants, many studies conducted with this compound show effects such as anti-inflammatory, anticancer, neuroprotective, antiproleferative, antimetastatic, antioxidant.[9] [10] Other studies have reported that ROS (Reactive Oxygen Species) is associated with some tumors such as colon cancer, hepatocellular carcinoma, leukemia, neuroblastoma, lung cancer and breast cancer.[11] [12] [13] [14] [15]

Rutin significantly inhibits the progression of HCC (Hepatocellular Carcinoma) cells, effective in colony migration and invasive potential of HEPG2 cells, is also a potent inhibitor of CYP3A4 and an activator of GSTP1 and NQ01.15 Likewise, rutin is a candidate drug in combination with other antitumor drugs, in addition, rutin can reduce drug resistance and side effects of chemotherapy.[16] The flavonoid rutin is commonly consumed in fruits, vegetables, vegetable drinks, in products whose formulations come in different presentations, either alone or in combination or with other ingredients that contain rutin.[17]

The sample of the species Ruta graveolans was collected at 4000 meters above sea level, from El Alto - La Paz, Bolivia. The present work shows the isolation of rutin (**1**) and 2-nonanone (**2**).

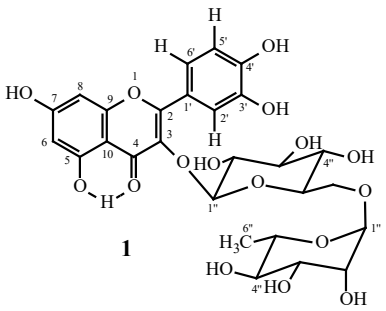

**1**

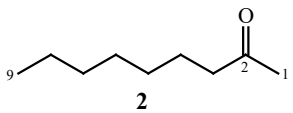

**2**

For the isolation of **1** a solid-liquid extraction of a dry sample was performed, using ethanol and water as solvents. Compound **2** was isolated through steam distillation of the aerial part of a dry sample. The isolated compounds were subjected to 1D-NMR, 2D-NMR and MS for their chemical identification, which were confirmed through a bibliographic comparison.

## RESULTS AND DISCUSSION

**Rutin (1).** The $^{1}$H NMR spectrum (DMSO-*d6*), Figure 1, shows signals at the following chemical shifts with their respective protons assigned to the flavonoid aglycone (quercetin): δ 6.19 ppm (H-6), δ 6.38 ppm (H-8), δ 6.85 ppm (H-5′), δ 7.55 ppm (H-2′), δ 7.53 ppm (H-6′). The anomeric protons of glucose and rhamnose appear at δ 5.35 ppm (H-1″) and δ 4.38 ppm (H-1‴), respectively. The protons between δ 3.04 ppm and δ 3.72 ppm correspond to H-5″, H-2″, H-5‴, and H-6″. The methyl group protons of rhamnose are observed at δ 1.05 ppm (H-6‴). Aromatic hydroxyl protons are seen at δ 12.60 ppm (OH-5), while other aromatic hydroxyl protons (OH-7, OH-3′, and OH-4′) appear between δ 8.7 ppm and δ 11.5 ppm. The aliphatic hydroxyl groups of the two sugars (OH-2″, OH-3″, OH-4″, OH-2‴, OH-3‴, and OH-4‴) are observed between δ 4.0 ppm and δ 5.6 ppm. These chemical shifts were compared with the literature as reported in Table 1. Figure 1a (see Reference Complement, rutin's $^{1}$H NMR spectrum, reproduced here from ref. 19,[19] (authorized reproduction pending from MDPI).

The $^{13}$C NMR spectrum (DMSO-$d_6$), Figure 2, shows the following chemical shifts corresponding to the aglycone: δ 156.85 ppm (C-2), δ 133.71 ppm (C-3), δ 177.78 ppm (C-4), δ 157.04 ppm (C-5), δ 99.11 ppm (C-6), δ 164.67 ppm (C-7), δ 94.04 ppm (C-8), δ 161.64 ppm (C-9), δ 104.37 ppm (C-10), δ 121.59 ppm (C-1′), δ 115.65 ppm (C-2′), δ 145.18 ppm (C-3′), δ 148.85 ppm (C-4′), δ 116.69 ppm (C-5′), δ 122.02 ppm (C-6′). For the 3-O-glucopyranoside: δ 101.59 ppm (C-1″), δ 74.50 ppm (C-2″), δ 76.86 ppm (C-3″), δ 70.43 ppm (C-4″), δ 76.50 ppm (C-5″), δ 67.44 ppm (C-6″). For the 6″-O-rhamnopyranosyl: δ 101.19 ppm (C-1‴), δ 70.80 ppm (C-2‴), δ 70.98 ppm (C-3‴), δ 72.26 ppm (C-4‴), δ 68.69 ppm (C-5‴), δ 18.18 ppm (C-6‴). These chemical shifts were compared with literature data corresponding to rutin, as shown in Table 1.

From the mass spectrum, in negative electrospray ionization mode, rutin primarily formed deprotonated molecular ions $[M–H]^-$ at m/z 611.25 in the full scan mass spectra. After optimizing the fragmentor voltage and collision energy, the dominant product ions for rutin were observed at m/z 465.15 and m/z 303.0, as shown in Figure 3. The fragmentation pattern of rutin is illustrated in Figure 4.

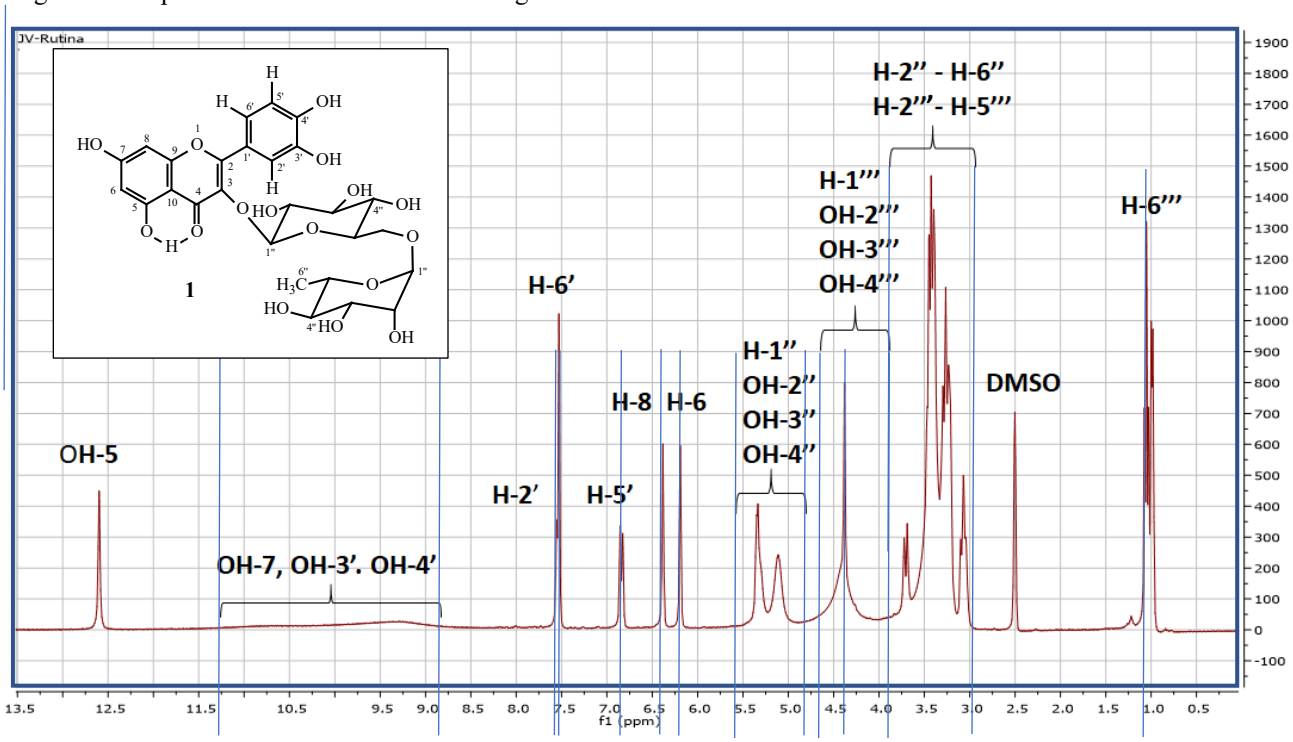


Fig. 1. $^{1}$H NMR Spectrum, rutin (DMSO-$d_6$, 300 MHz)

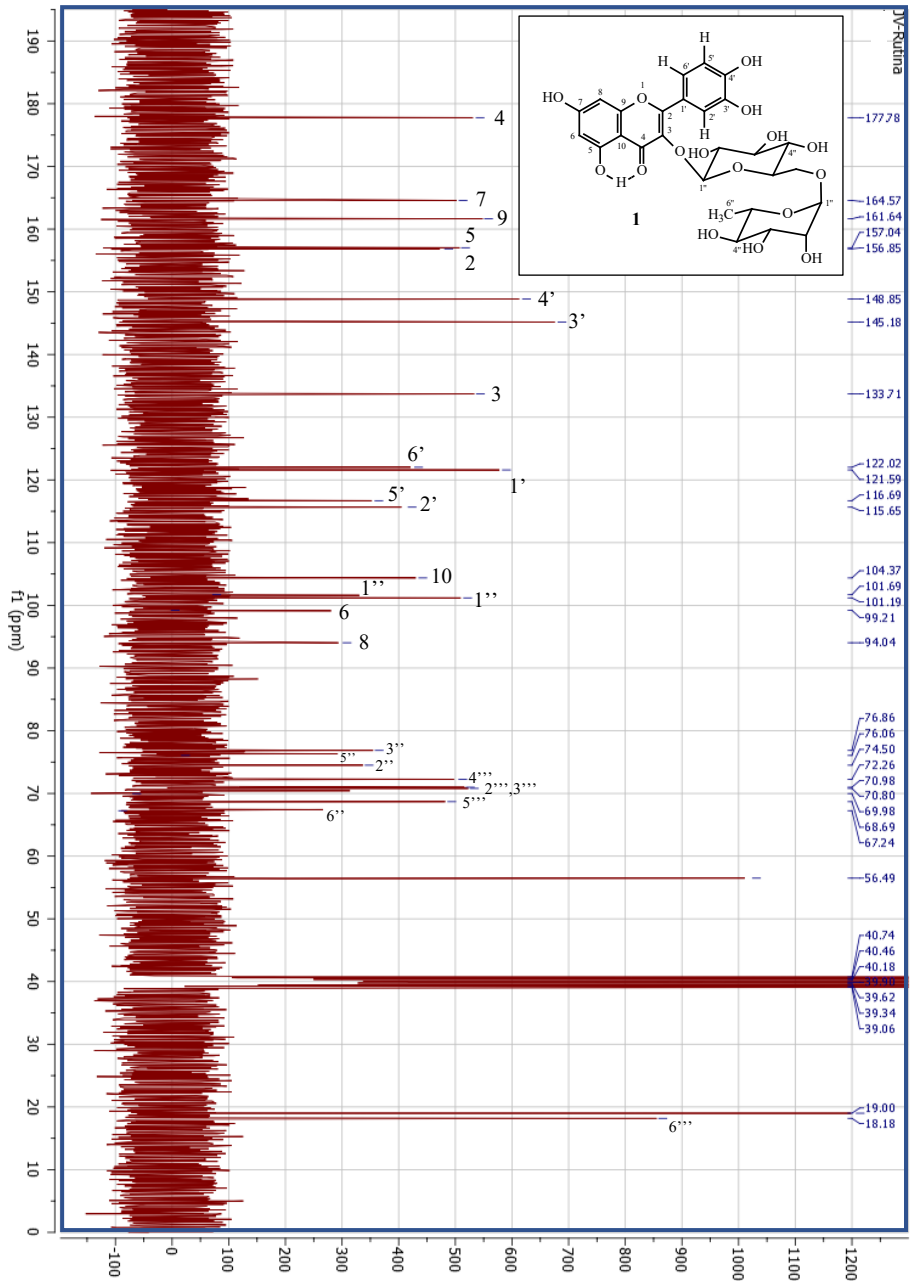


Fig. 2. $^{13}$C NMR Spectrum, rutin (DMSO-$d_6$, 75 MHz)

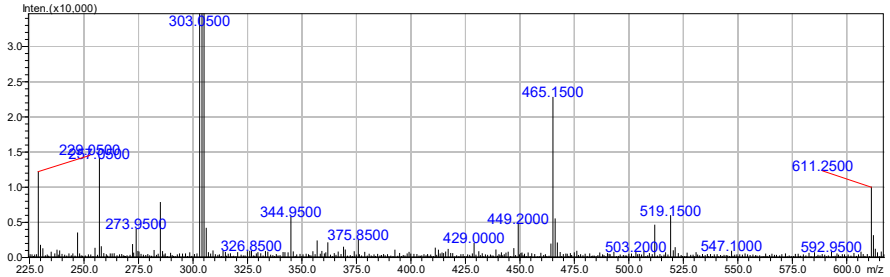


Fig. 3. LC-ESI-MS (-4.5 kV) spectrum, rutin

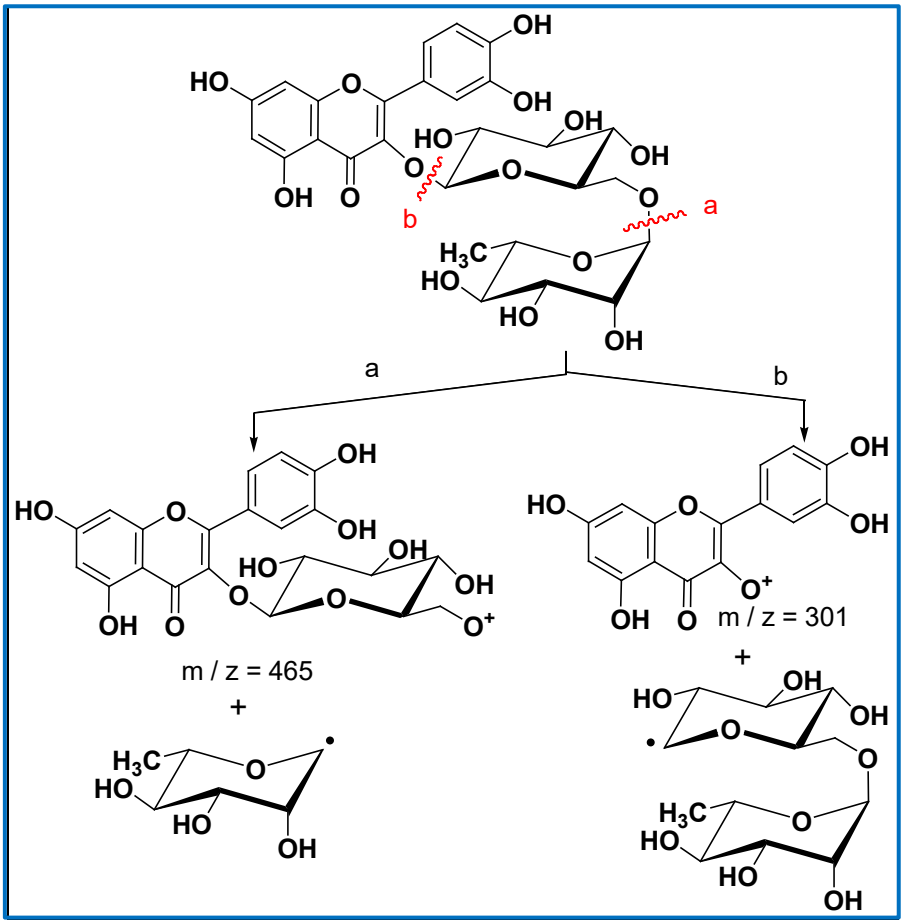


Fig. 4. EIMS (LC-ESI-MS) fragmentation pattern, rutin

**2-Nonanone (2).** The $^{1}$H NMR spectrum ($CDCl_3$) shown in Figure 5 displays five signal regions:

- At δ 0.74 ppm, corresponding to three methyl proton groups
- At δ 1.12 ppm, indicating the presence of ten methylene protons
- At δ 1.40 ppm, corresponding to two methylene protons
- At δ 1.96 ppm, associated with three methyl protons
- At δ 2.25 ppm, corresponding to two methylene protons

The $^{13}$C NMR spectrum ($CDCl_3$), as shown in Figure 6, reveals nine carbon signals at: δ 208.45 ppm, δ 43.31 ppm, δ 31.44 ppm, δ 29.14 ppm, δ 29.29 ppm, δ 28.89 ppm, δ 23.49 ppm, δ 22.24 ppm, and δ 13.67 ppm.

From the DEPT-135 experiment (Figure 6), the spectrum shows:

- One quaternary carbon at δ 208.45 ppm
- Two methyl groups at δ 29.29 ppm and δ 13.67 ppm
- Six methylene groups at δ 43.31 ppm, δ 23.49 ppm, δ 28.89 ppm, δ 29.14 ppm, δ 31.44 ppm, and δ 22.24 ppm

In the COSY $^{1H-1}$H experiment (Figure 7):

- The methyl protons at δ 0.72 ppm correlate with the methylene protons at δ 1.12 ppm
- The methylene protons at δ 1.11 ppm correlate with those at δ 1.40 ppm
- The methylene protons at δ 1.40 ppm correlate with those at δ 2.25 ppm

These correlations are illustrated in Figure 8. The chemical shifts were compared with literature reports for $^{1}H$ and $^{13}C$ NMR spectra, [18] [19] [20] [21], as shown in Tables 2 and 3.

The mass spectrum of 2-nonanone is shown in Figure 9, where a peak at m/z 58 is observed due to a rearrangement consistent with the McLafferty mechanism. The most intense peak at m/z 43 results from an alpha (α) cleavage on the more substituted side of the carbonyl group. Another cleavage produces a peak at m/z 71, corresponding to a gamma (γ) cleavage on the more substituted side of the carbonyl group. It is also worth noting that the peak at m/z 142 is very small. These cleavages and the McLafferty rearrangement are depicted in Figure 10.

Table 1. $^{1}H$,$^{13}C$ NMR chemical shifts of rutin, experimental and reported, compared

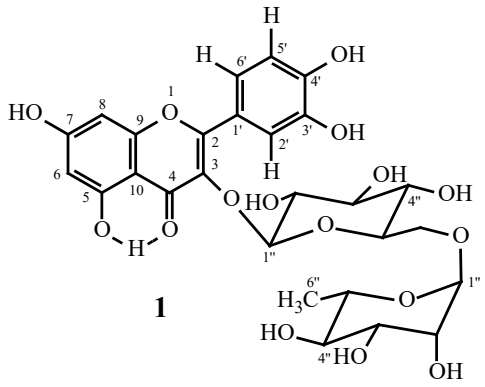

**1**

| Atom | (1) δH ppm *m* ($J_{Hz}$) DMSO-$d_6$ 300MHz | Rutin[18] δH ppm *m* ($J_{Hz}$) DMSO-$d_6$ 400 MHz | Rutin [19] δH ppm *m* DMSO-$d_6$ 400 MHz | Rutin[20] δH ppm *m* ($J_{Hz}$) $CD_3OD$ 600 MHz | (1) δC ppm DMSO-$d_6$ 75 MHz | Rutin[18] δC ppm DMSO-$d_6$ 100 MHz | Rutin[21] δH/C ppm $CD_3OD$ 700 MHz |
|---|---|---|---|---|---|---|---|
| **Aglycone** | | | | | | | |
| 2 | - | - | - | - | 156.85 | 156.6 | - / 158.50 |
| 3 | - | - | - | - | 133.71 | 133.3 | - / 135.72 |
| 4 | - | - | - | - | 177.78 | 179.4 | - / 179.41 |
| 5-OH | 12.60 *s* | - | 12.60 *s* | - | 157.04 | 161.3 | - / 163.00 |
| 6 | 6.19 *brs* | 6.201 *d* (2.1) | 6.20 *s* | 6.19 *d* (1.8) | 99.21 | 98.7 | 6.21 / 100.01 |
| 7 | - | - | - | | 164.57 | 164.0 | - / 166.13 |
| 8 | 6.38 *brs* | 6.404 *d* (2.1) | 6.45 *s* | 6.38 *d* (2.4) | 94.04 | 93.6 | 6.37 / 95.00 |
| 9 | - | - | - | | 161.64 | 156.4 | - / 159.44 |
| 10 | - | - | - | | 104.37 | 104.0 | - / 105.72 |
| 1’ | - | - | - | | 121.59 | 121.2 | - / 123.72 |
| 2’ | 7.55 *d* (2.0) | 7.573 *d* (2.1) | 7.55 *d* | 7.66 *d* (1.8) | 115.65 | 115.2 | 7.67 / 117.63 |
| 3’ | - | - | - | | 145.18 | 144.8 | - / 145.92 |
| 4’ | - | - | - | | 148.85 | 148.4 | - / 149.92 |
| 5´ | 6.85 *d* (9.0) | 6.874 *d* (9.0) | 6.90 | 6.86 *d* (8.5) | 116.69 | 116.3 | 6.88 / 116.01 |
| 6’ | 7.53 *d* (9.0) | 7.548 *dd* (9.0, 2.1) | 7.53 *d* | 7.64 *dd* (8.5, 1.8) | 122.02 | 121.6 | 7.63 / 123.65 |
| OH-7, 3’, 4’ | 8.80-11.50 *m* | | 8.80-11.50 *m* | | | | |
| **β-D-glu** | | | | | | | |
| 1’’ | 5.35 *brs* | 5.375 *d* (7.5) | 5.35 *d* | 5.10 *d* (7.9) | 101.69 | 101.2 | 5.11 / 104.72 |
| 2’’ | 3.35 *m* | 3.071-3.710 *m* | 3.35 *m* | 3.46 *dd* (9.8, 7.5) | 74.50 | 74.1 | 3.47 / 75.84 |
| 3’’ | 3.35 *m* | 3.071-3.710 *m* | 3.35 *m* | 3.25 *t* (9.8) | 76.86 | 76.5 | 3.41 / 78.02 |
| 4’’ | 3.35 *m* | 3.071-3.710 *m* | 3.35 *m* | 3.29 | - | 70.0 | 3.26 / 71.11 |
| 5’’ | 3.35 *m* | 3.071-3.710 *m* | 3.35 *m* | 3.38 *m* | 76.06 | 75.9 | 3.32 / 77.52 |
| 6’’ | 3.35 *m* | 3.071-3.710 *m* | 3.35 *m* | 3.79 *dd* (11.0,1.2) **a** | 67.24 | 66.9 | 3.39 **a** / 68.60 |
| OH-2’’, 3’’, 4’’ | 5.50-5.00 *m* | | 4.45 *m* | 3.63 *dd* (12.0, 4.9) **b** | | | 3.80 **b** |
| **α-L-rha** | | | | | | | |
| 1’’’ | 4.38 *brs* | 4.400 *d* (2.0) | 4.40 *s* | 4.51 *d* (1.8) | 101.19 | 100.8 | 4.52 / 102.54 |
| 2’’’ | 3.35 *m* | 3.071-3.710 *m* | 3.35 *m* | 3.63 *dd* (3.7, 1.8) | 70.80 | 70.4 | 3.63 / 72.32 |
| 3’’’ | 3.35 *m* | 3.071-3.710 *m* | 3.35 *m* | 3.53 *dd* (9.8, 3.7) | 70.98 | 70.6 | 3.54 / 72.44 |
| 4’’’ | 3.35 *m* | 3.071-3.710 *m* | 3.35 *m* | 3.28 *t* (9.8) | 72.26 | 71.9 | 3.28 / 73.91 |
| 5’’’ | 3.35 *m* | 3.071-3.710 *m* | 3.35 *m* | 3.43 *m* | 68.69 | 68.2 | 3.45 / 69.80 |
| 6’’’ | 1.05 *d* (6.0) | 1.022 *d* (6.3) | 1.00 *d* (6.0) | 1.12 *d* (6.7) | 18.18 | 17.7 | 1.12 / 18.04 |
| OH-2’’’, 3’’’, 4’’’ | 4.62-3.90 *m* | | 4.75-4.25 | | | | |

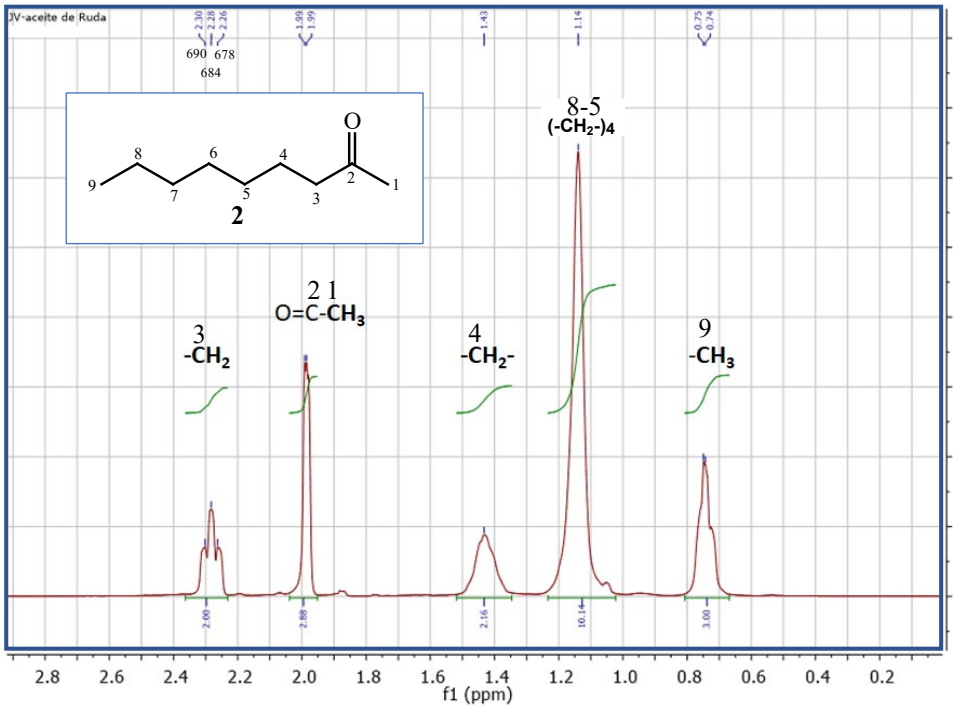


Fig. 5. $^{1}$H NMR spectrum, 2-nonanone (DMSO-$d_6$, 300 MHz)

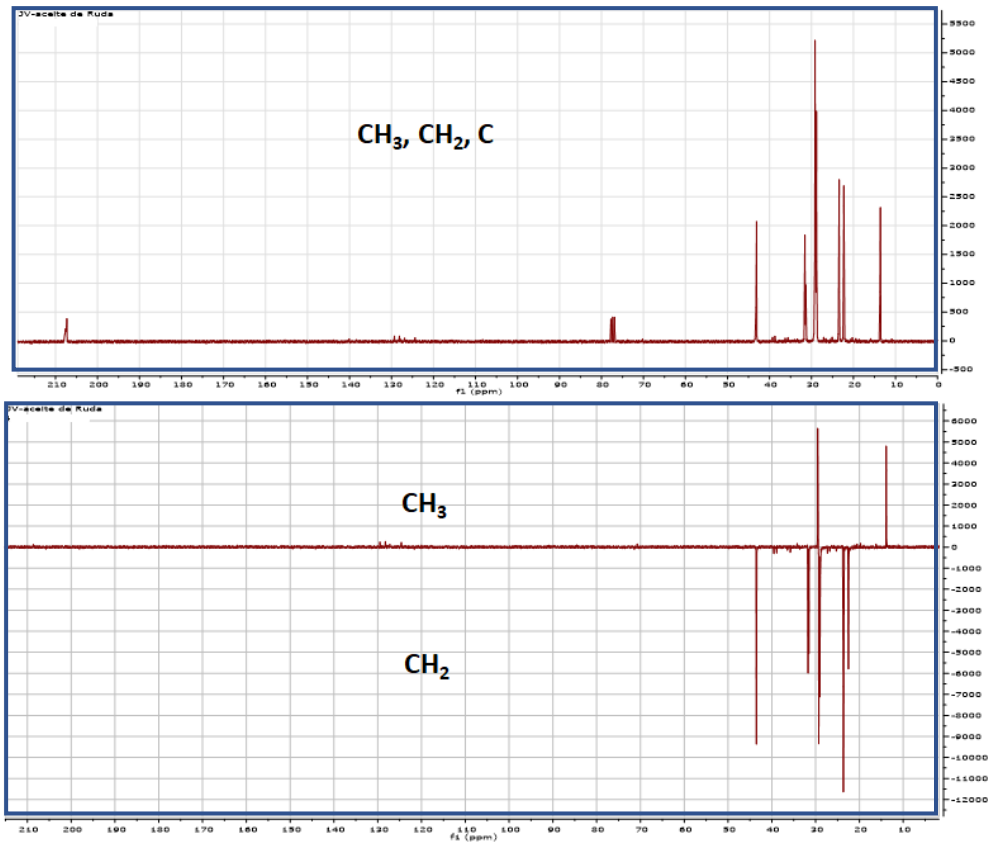


Fig. 6. $^{13}$C and DEPT-135 NMR spectra, 2-nonanone (DMSO-$d_6$, 75 MHz)

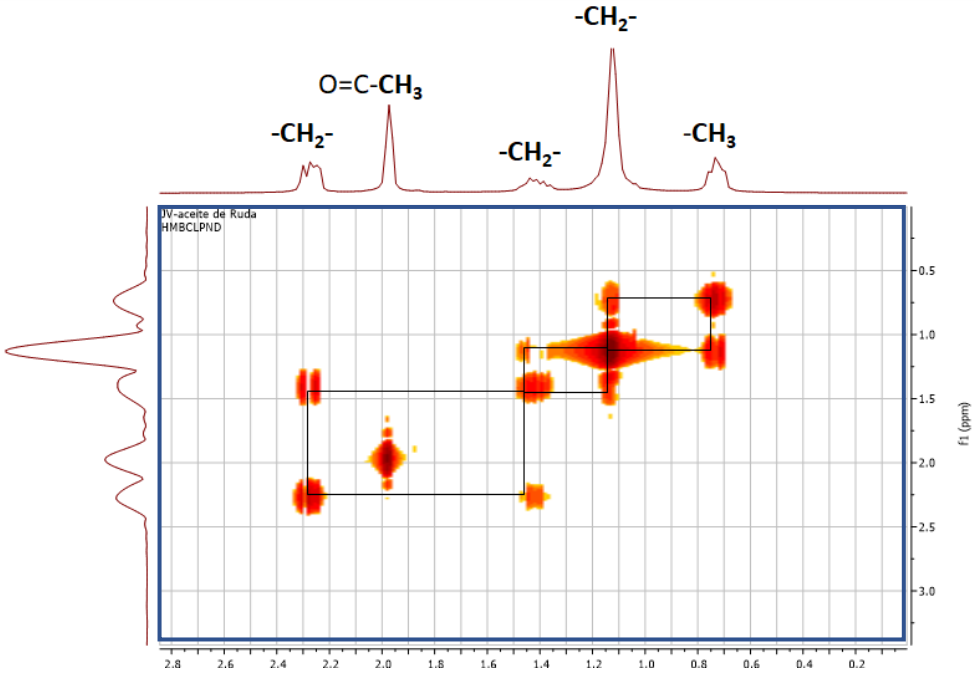


Fig. 7. COSY experiment, 2-nonanone

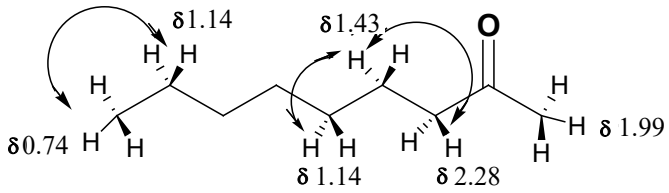


Fig. 8. COSY correlation, 2-nonanone

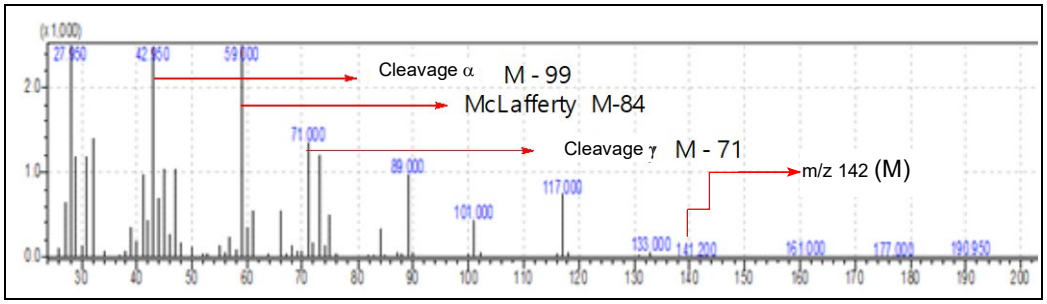


Fig. 9. GC/EIMS (70 eV) spectrum, 2-nonanone

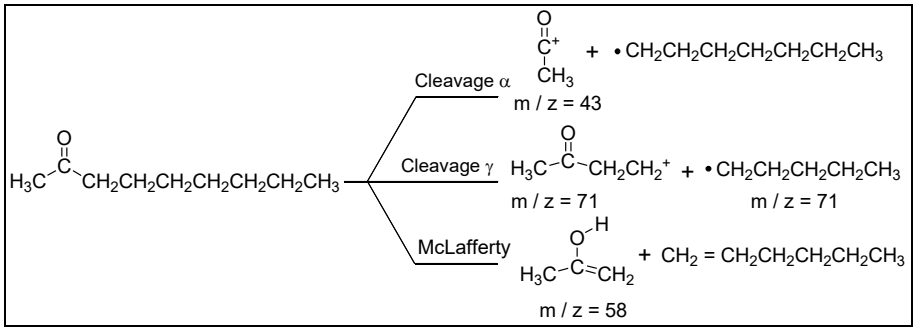


Fig. 10. EIMS fragmentation pattern of 2-nonanone

The purpose of the study is to determine the spatial structure and conformations of 2-nonanone in gas phase were performed by B3LYP/6-31G* method. 248 conformers (at least) can be determined out of calculations using our current-use method. A significant rotational energy barrier is the main key in conformational study. As Figure 11 shows the 4 dimensional structure of 2-nonanone conformers in gas phase and shows four minimum energy points named N1, N2. N3 and N4. The most stable conformer is N1.

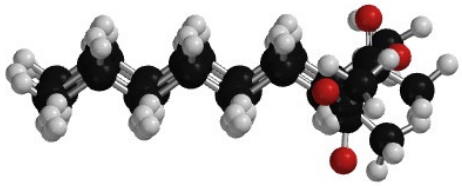

Fig. 11. Four conformers (N1, N2, N3, N4) of 2-nonanone

By applying B3LYP/6-31G* method, $^{1}$H NMR and $^{13}$C NMR chemical shifts were measured for N1 to N4 in gas phase and were compared to TMS shift. Tables 2 and 3 show the experimental and theoretical comparison the hydrogen and carbon chemical shifts for N1 to N4 conformers, respectively. From energy differences and chemical shifts, it can be concluded that N1 conformer has a higher natural population, compared to other conformers; therefore, the calculated chemical shifts for N1 are closer to experimental results. The Correlation between the experimental $^{13}$C NMR chemical shifts and the computed $^{13}$C NMR chemical shifts as calculated to N1, N2, N3 and N4 shows in the figure 12. Excellent linear regression correlation coefficient ($R^2 > 0.9977–0.9986$) is obtained N1 to N4. Energy scanning calculations around - dihedral angle ($C_1$-$C_2$-$C_3$-$C_4$) show meaningful energy barriers and, subsequently, stable conformers. The four conformers have different dihedral angle with show in the table 4.

Table 2. Comparison of experimental ($CHCl_3$ solvent), Reference[22] and theoretical 6-31G* (Spartan 18) $^{1}$H NMR chemical shifts (ppm), 2-nonanone

| Atom | H | $\delta_H$ (ppm) Exp. | $\delta_H$ (ppm) [22] | $\delta_H$ (ppm) Calc. N1 | $\delta_H$ (ppm) Calc. N2 | $\delta_H$ (ppm) Calc. N3 | $\delta_H$ (ppm) Calc. N4 |
|---|---|---|---|---|---|---|---|
| **1** | $CH_3$ | 1.96 | 2.13 | 1.9 | 1.9 | 1.9 | 1,9 |
| **2** | CO | - | - | - | - | - | - |
| **3** | $CH_2$ | 2.25 | 2.40 | 2.3 | 2.3 | 2.2 | 2.2 |
| **4** | $CH_2$ | 1.40 | 1.57 | 1.6 | 1.5 | 1.6 | 1.5 |
| **5** | $CH_2$ | 1.12 | 1.27 | 1.2 | 1.3 | 1.3 | 1.4 |
| **6** | $CH_2$ | 1.11 | 1.27 | 1.4 | 1.4 | 1.3 | 1.4 |
| **7** | $CH_2$ | 1.11 | 1.27 | 1.3 | 1.3 | 1.3 | 1.4 |
| **8** | $CH_2$ | 1.12 | 1.27 | 1.4 | 1.4 | 1.4 | 1.4 |
| **9** | $CH_3$ | 0.72 | 0.88 | 0.9 | 0.9 | 0.9 | 1.0 |

Table 3. Comparison of experimental ($CHCl_3$ solvent), Reference[23] and theoretical 6-31G* (Spartan 18) $^{13}$C NMR chemical shifts (ppm)

| Atom | C | $\delta_C$ (ppm) Exp. | $\delta_C$ (ppm) [23] | $\delta_C$ (ppm) Calc. N1 | $\delta_C$ (ppm) Calc. N2 | $\delta_C$ (ppm) Calc. N3 | $\delta_C$ (ppm) Calc. N4 |
|---|---|---|---|---|---|---|---|
| **1** | $CH_3$ | 29.29 | 29.26 | 27.2 | 27.7 | 24.3 | 25.6 |
| **2** | CO | 208.45 | 208.85 | 209.1 | 209.1 | 211.1 | 211.1 |
| **3** | $CH_2$ | 43.31 | 43.85 | 41.3 | 39.1 | 42.4 | 43.2 |
| **4** | $CH_2$ | 23.49 | 24.01 | 26.7 | 25.4 | 28.1 | 29.2 |
| **5** | $CH_2$ | 28.89 | 29.26 | 32.1 | 31.4 | 30.8 | 33.5 |
| **6** | $CH_2$ | 29.14 | 29.75 | 33.0 | 33.0 | 33.1 | 32.9 |
| **7** | $CH_2$ | 31.44 | 31.84 | 34.4 | 34.2 | 33.9 | 34.1 |
| **8** | $CH_2$ | 22.24 | 22.73 | 25.5 | 25.5 | 25.5 | 25.5 |
| **9** | $CH_3$ | 13.67 | 14.08 | 15.8 | 15.8 | 15.7 | 15.8 |

Table 4. calculations dihedral angle (β) $C_1$-$C_2$-$C_3$-$C_4$ from conformers N1, N2, N3 and N4, 2-nonanone

| Dihedral angles (β) | Conformer N1 | Conformer N2 | Conformer N3 | Conformer N4 |
|---|---|---|---|---|
| $C_1$-$C_2$-$C_3$-$C_4$ | 180.00 | 170.78 | -68.91 | -79.98 |

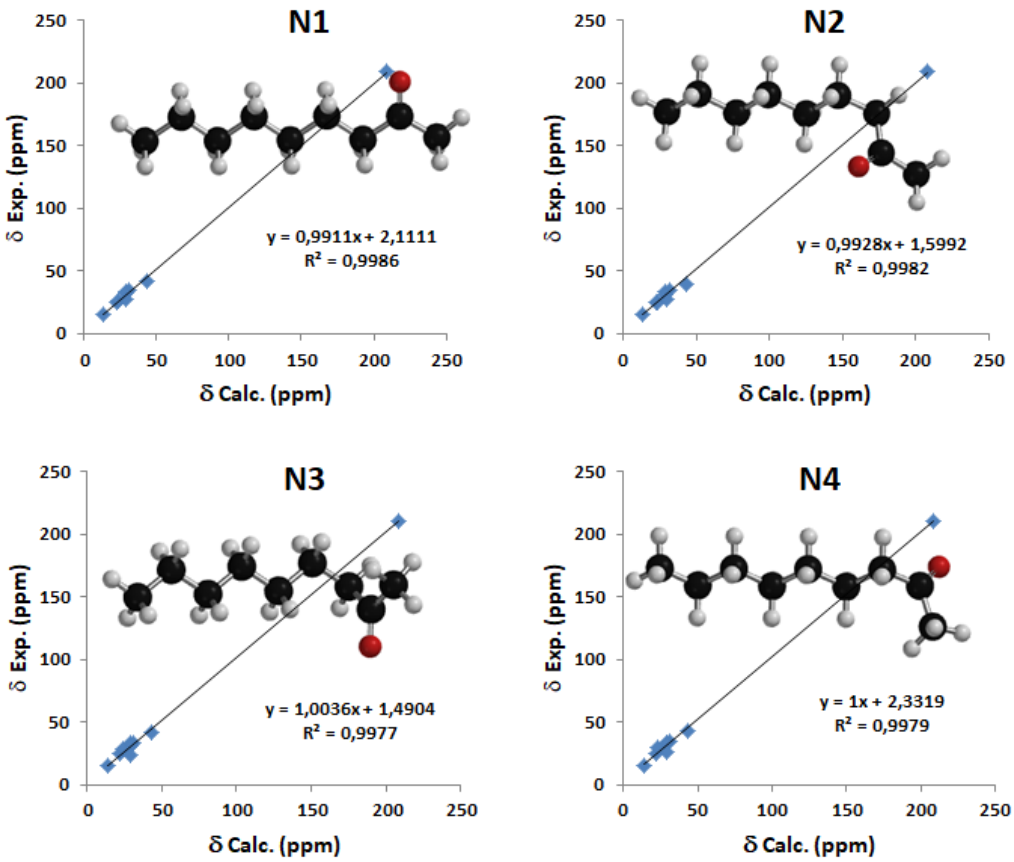


Fig. 12. Correlation between the experimental chemical shifts and the computed chemical shifts using B3LYP/6-31G* for $^{13}C$ NMR, 2-Non

## EXPERIMENTAL

### General

***Nuclear Magnetic Resonance Spectroscopy***

The NMR spectra were recorded on a Bruker DRX300 NMR spectrometer (300 MHz, 75 MHz) using TMS as the internal standard at IIQ-UMSA. Chemical shifts, in ppm, are referenced to TMS. The following measurement techniques were employed: standard $^{1}H$, Attached Proton Test (APT, not shown), Correlation Spectroscopy (COSY), $^{13}C$ NMR, and DEPT-135.

***Computational Methodology***

The calculation of $^{1}H$ and $^{13}C$ NMR chemical shifts, dihedral angles, optimized geometries, and statistical validation of theoretical NMR shifts based on experimental data were performed using B3LYP/6-31G* with Spartan 18 software, for 2-nonanone.

### Plant material

The sample of the species *Ruta graveolans* was collected at 4000 m.a.s.l., at El Alto - La Paz, Bolivia in 1999. The herbarium specimen was identified by specialists at the National Herbarium of Bolivia (LPB, director: Dr. Stephan Beck) and is deposited at LPB with the label JVRG-1.

### Isolation of compounds

***Rutin (1)***

A quantity of 40.85 g of dry sample was reduced in size and brought into contact with $C_2H_5OH/H_2O$ in a volume ratio of 1:5. A solid–liquid extraction was carried out over a period of 48 hours, after which the solvent was removed using a rotary evaporator, leaving behind a yellow-colored solid residue. This solid was dried and recrystallized in

$C_2H_5OH/H_2O$ at a ratio of 3:1, yielding a yellow solid in a quantity of 1.03 g. The product was subjected to $^1H$ NMR, $^{13}C$ NMR, and mass spectrometry. The chemical structure was compared with bibliograpy (see Table 1).

***2-Nonanone (2)***

From a quantity of 201 g of dry sample, which was reduced in size and placed in a conventional steam distillation apparatus for 3 hours, the resulting oil was separated from the aqueous solution, yielding 0.3 mL of essential oil. This oil was dried with anhydrous sodium sulfate and stored in amber vials under refrigeration. The obtained oil was analyzed using $^1H$ NMR, $^{13}C$ NMR, DEPT-135, COSY $^1H$–$^1H$, and mass spectrometry. The identification of 2-nonanone was carried out through interpretation of 1D and 2D NMR spectroscopic data, mass spectrometry, and comparison with literature sources.[24 25]

**Physicochemical data of 1 and 2**

***Rutin (1)***

LC-ESI-MS negative mode, 4.5 kV; *m/z* (Rel. %): 611.25 (28.6%, $[M–H]^-$), 465.15 (64.3%), 303.0 (100%). $^1H$ NMR 300 MHz (DMSO-$d_6$): see Table 1.; $^{13}C$ NMR 75 MHz (DMSO-$d_6$): see Table 1.

***2-Nonanone (2)***

GC/EIMS, 70 eV; *m/z* (Rel.%): 141.200 (0.1%, $[M–H]^+$]), 133.000 (1%), 117.000 (28 %), 101.00 (28 %), 89.000 (40%), 71.000 (56%, $[M–71]^+$, cleavage γ), 59.000 (100%, $[M–84]^+$, McL), 42.950 (100%, $[M–99]^+$, cleavage α), 27.950 (100%). $^1H$ NMR 300 MHz ($CDCl_3$): δ 0.74 (t, 3H, H-9), 1.14 (m, 8H, H-5–H-8), 1.43 (quintet, 2H, H-4), 1.99 (s, 3H, H-1), 2.28 (t, $J$ = 6 Hz, 2H, H-3). $^{13}C$ NMR 75 MHz ($CDCl_3$): δ 208.45, 43.31, 31.44, 29.14, 29.29, 28.89, 23.49, 22.24, 13.67.

**Mass Spectroscopy (MS)**

***Rutin - LCMS analysis conditions***

1 mg of the sample was dissolved in chromatographic-grade methanol and subsequently filtered through a 0.22 µm PTFE filter. To obtain the mass spectrum of the isolated molecule (rutin), the LC-ESI-MS high-pressure chromatography system (LCMS-2020; Shimadzu) was used, employing a 250 mm C18 column (4.6 mm i.d. and 5 µm particle size; RESTEK). Mobile phase A (0.1% formic acid in water) and mobile phase B (acetonitrile) were used for separation. The concentration of mobile phase B was programmed to 20% (0 min) – 20% (5 min) – 80% (25 min). The column temperature was 30 °C. For ESI ionization mode, 4.5 kV was used for the positive ion mode and -4.5 kV for the negative ion mode.

***2-nonanone - GC/MS analysis conditions***

For sample identification, a SHIMADZU GC 2010 PLUS gas chromatograph coupled to a SHIMADZU QP 2020 mass spectrometer was used. Separation of the compounds was performed using a RESTEK Rxi-5Sil MS column containing 5% diphenyl and 95% dimethylpolysiloxane (30 m x 0.25 mm and 0.25 µm film thickness). The injection volume was 1 µL at a total flow rate of 4.2 mL/min, and the column flow rate was 0.59 mL/min. The injector temperature was 250 °C. The initial temperature in the oven was 50 °C, maintained for 5 min, and subsequently increased to 260 °C at a rate of 15 °C/min for 5 min. The ionization temperature used was 250 °C and the interface temperature was 280 °C.

**Reference supplemental[19]**

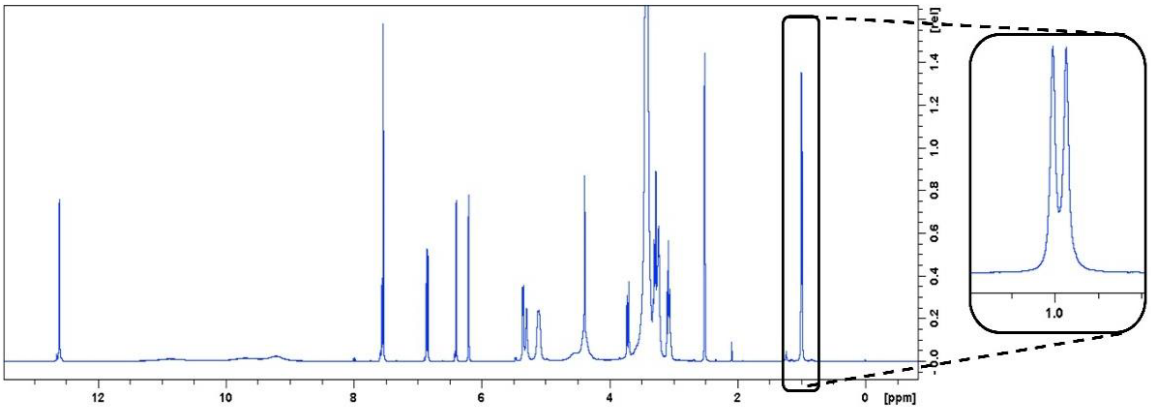


Fig. 1a. $^1H$ NMR spectrum of Rutin; 400 MHz (DMSO-$d_6$), (A. Parra-Naranjo et al.[19]); authorized reproduction pending from MDPI *Molecules*

## REFERENCES

[1] L. Girault, 'Kallawaya, Curanderos Itinerantes de los Andes: investigación sobre prácticas medicinales y mágicas'. Edit. Quipus, La Paz, 1987.
[2] A. A. Pollio, E. De Natale, G. Appetiti, A. Aliotta, A. Touwaide, *J. Etnofarmacol*. 2008, **116**, 469. https://doi.org/10.1016/j.jep.2007.12.013
[3] A. T. Coimbra, S. Ferreira, A. P. Duarte, *J. Ethnopharmacol.*, 2020, **260**, 113076. doi: 10.1016/j.jep.2020.113076. DOI: 10.1016/j.jep.2020.113076
[4] R. Quiroga, L. Meneses, R. W. Bussmann, *Journal of ethnobiology and ethnomedicine*, 2012, **8**, 29. https://doi.org/10.1186/1746-4269-8-29
[5] L. Nahar, H. R. El-Seedi, S. A. M. Khalifa, M. Mohammadhosseini, S. D. Sarker, *Molecules*, 2021, **26**, 4766, https://doi.org/10.3390/molecules26164766
[6] I. N. Kuzovkina, S. Szarka, E. Hethelyi, E. Lemberkovics, E. Szoke, *Russ. J. Plant. Physiol*., 2009, **56**, 846. https://doi.org/10.1134/S1021443709060156
[7] T. Amdouni, S. B. Abdallah, N. Msilini, F. Merck, M. Chebbi, M. Lachaal, N. Karray-Bouraoui, Z. Ouerghi, X. Fernandez, *Acta Physiol. Planta* 2016, **38**, 147. https://doi.org/10.1007/s11738-016-2167-x
[8] Z. Bennaoum, H. Benhassini, D. Falconieri, A. Piras, S. Porcedda, *Nat. Prod. Res.*, 2017, **31**, 2329. https://doi.org/10.1080/14786419.2017.1303692
[9] A. Satari, S. A. Amini, E. Raeisi, Y. Lemoigne, and E. Hiedarian, *Advanced Pharmaceutical Bulletin*, 2019, **9**, 462. DOI: 10.15171/apb.2019.055
[10] C. Wang, S. Shang, X. Zheng et al., *Journal of the Brazilian Chemical Society*, 2019, **30**, 988. https://web.archive.org/web/20200209192914/http://static.sites.sbq.org.br/jbcs.sbq.org.br/pdf/2018-0325AR.pdf
[11] A. Ganeshpurkar and A. K. Saluja, *Saudi Pharmaceutical Journal*, 2017, **25**, 149. DOI: 10.1016/j.jsps.2016.04.025
[12] A. Annapurna, C. S. Reddy, R. B. Akondi, and S. R. C. Rao, *Journal of Pharmacy and Pharmacology*, 2009, **61**, 1365. DOI: 10.1211/jpp/61.10.0014
[13] A. J. Alonso-Castro, F. Dom, and A. Garc, *Archives of Medical Research*, 2013, **44**, 346. DOI: 10.1016/j.arcmed.2013.06.002
[14] M. Sathiya, R. Tangam, T. Salammal, R. Sasirekha, S. Sivasubramanian, and M. Dinesh, *Biomedicine & Pharmacotherapy*, 2019, **109**, 1181. https://doi.org/10.1016/j.biopha.2018.10.178.
[15] S. S. Choi, H. R. Park and K. A. Lee, *Antioxidants* 2021, **10**, 1696. https://doi.org/10.3390/antiox10111696.
[16] S. Karakurt, *Acta Pharm.*, 2016, **66**, 49. https://doi.org/10.1515/acph-2016-0046
[17] A. Satari, S. Ghasemi, S. Habtemariam, S. Asgharian, and Z. Lorigooini, *Evidence-Based Complementary and Alternative Medicine*, 2021, 9913179. https://doi.org/10.1155/2021/9913179
[18] A. H. Sheded, M. A. EL-Hashash, S. A. EL-Toumy, J. Y. Salib, S. William, M. M. Hamed, *Egyptian Jounal of Chemistry*, 2021, **64**, 4557.https://ejchem.journals.ekb.eg/article_185441_9cf3bdea7834baa2a3e5db4a9f9b9422.pdf
[19] A. Parra-Naranjo, C. Delgado-Montemayor, R. Salazar-Aranda, R. Castro-Ríos, A. L. Saucedo, and N. Waksman-Minsky, *Molecules*, 2022, **27**, 6593. https://doi.org/10.3390/molecules27196593
[20] M. Zor, S. Aydin, N.D. Güner, N. Başaran and A. A. Başara*n, BMC Complement Altern Med,* 2017 **17**, , 229. https://doi.org/10.1186/s12906-017-1732-1
[21] M. Forino, L. Tartaglione, C. Dell'Aversano, P. Ciminiello, *Food Chemistry*, 2016, **194**, 1254. https://doi.org/10.1016/j.foodchem.2015.08.129
[22] https://sdbs.db.aist.go.jp/HNmrSpectralView.aspx?imgdir=hsp&fname=HSP01496&sdbsno=2134. Access date: March 2025
[23]https://sdbs.db.aist.go.jp/CNmrSpectralView.aspx?imgdir=cds&fname=CDS00509&sdbsno=2134. Access date: March 2025
[24] https://www.chemicalbook.com/SpectrumEN_821-55-6_1HNMR.htm. Access date: March 2025
[25] https://www.chemicalbook.com/SpectrumEN_821-55-6_13CNMR.htm. Access date: March 2025